CHEMISTRY
A EUROPEAN JOURNAL

FULL PAPER

DOI: 10.1002/chem.201200225

Coordination Studies on Supramolecular Chiral Ligands and Application in Asymmetric Hydroformylation

Rosalba Bellini and Joost N. H. Reek*[a]

Dedicated to Professor Dr. Piet van Leeuwen on the occasion of his 70th birthday

Abstract: In this study we introduce a series of monodentate pyridine-based ligands for which the phosphorus coordination mode to rhodium can be controlled by the binding of Zn^{II}-templates to the pyridyl group. A series of monodentate phosphoroamidite and phosphite ligands have been prepared and studied under hydroformylation conditions by in situ high-pressure NMR and IR techniques. These studies reveal the exclusive formation of rhodium hydride complexes in which the phosphorus atom of the ligand resides in an axial position, *trans* to the hydride, but only after addition of Zn^{II}-template. In the absence of these templates the usual mono-coordinated rhodium hydrido complexes are formed, with the phosphorus ligated in the equatorial plane, *cis* to the hydride. The catalytic performance of these complexes is evaluated in asymmetric hydroformylation of unfunctionalised internal alkenes in which the supramolecular change is reflected in higher activity and selectivity.

Keywords: alkenes · coordination modes · hydroformylation · molecular recognition · supramolecular chemistry

Introduction

The influence of ligands on the structure and performance of catalytically active metal complexes has been intensely studied in coordination and organometallic chemistry.[1] A tremendous amount of research has been devoted to ligand design to control coordination chemistry, which is leading to new approaches in catalyst development. In modern coordination chemistry the use of highly advanced in situ spectroscopic techniques (high-pressure (HP) spectroscopy, for example, HP NMR and HP IR) has enabled scientists to observe the formation of active species and the resting state under relevant reaction conditions.[2,3] These spectroscopic techniques have been widely used as tools for the identification of catalytic intermediates and resting states, particularly for the development of phosphine-based rhodium complexes for hydroformylation reactions.[3]

The active species in this reaction has been determined to be trigonal bipyramidal complexes in which the hydride ligand resides on the axial position and the phosphorus ligands are either coordinated in the equatorial–equatorial (eq–eq) or in the equatorial–axial (eq–ax) mode (Figure 1).

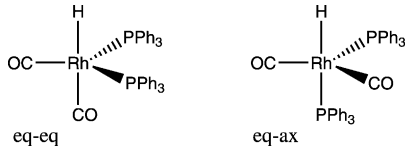

Figure 1. Different coordination modes of triphenylphosphine rhodium catalyst.

For bidentate ligands, van Leeuwen and co-workers evaluated the effect of the natural bite angle on the selectivity and activity in the rhodium-catalysed hydroformylation reaction using a series of diphosphine ligands based on a xanthene-type backbone.[4] These studies showed that bidentate phosphorus ligands with wide bite angles predominantly promote the formation of the eq–eq rhodium complex. In addition, these complexes are highly selective in the rhodium-catalysed hydroformylation of 1-octene, yielding the linear aldehyde product.[4] Coordination behaviour of bidentate ligands also appears to be crucial for asymmetric hydroformylation. Most significant advances in the field of asymmetric hydroformylation have been obtained with catalytic systems that are based on hybrid phosphine–phosphite or phosphine–phosphoroamidite ligands.[5] A historically important breakthrough was reported by Takaya and Nozaki who described the use of Binaphos rhodium complexes to generate enantiomeric excesses of up to 95% for a large variety of substrates.[6] The reason for the exceptionally high enantioselectivity was attributed to the exclusive formation of a single active species in which the ligand preferentially coordinates to the transition metal centre in an eq–ax fashion.[6]

[a] R. Bellini, Prof. Dr. J. N. H. Reek
Van't Hoff Institute for Molecular Sciences
University of Amsterdam
Science Park 904, 1098 XH, Amsterdam (The Netherlands)
Fax: (+31) 205255604
E-mail: j.n.h.reek@uva.nl
Homepage: http//www.science.uva.nl/research/imc/Homkat/

Supporting information for this article is available on the WWW under http://dx.doi.org/10.1002/chem.201200225.

Monodentate ligands have rarely been applied in asymmetric hydroformylation reactions because low selectivities are anticipated due to lower control over coordination modes. However, breakthroughs in this area would be interesting because these monodentate ligands have a simple structure and, hence, their synthesis is generally much less elaborate. This makes them potentially cheaper and the preparation of large ligand libraries is easier, which is crucial for combinatorial approaches to find new active and selective catalysts.[7] The application of very bulky monodentate phosphite (π-accepting) ligands have been studied with the aim of generating highly active rather than enantioselective catalysts. It has been demonstrated that these do indeed form very active hydroformylation catalysts, even for the less reactive internal alkenes, albeit with significant isomerisation.[8]

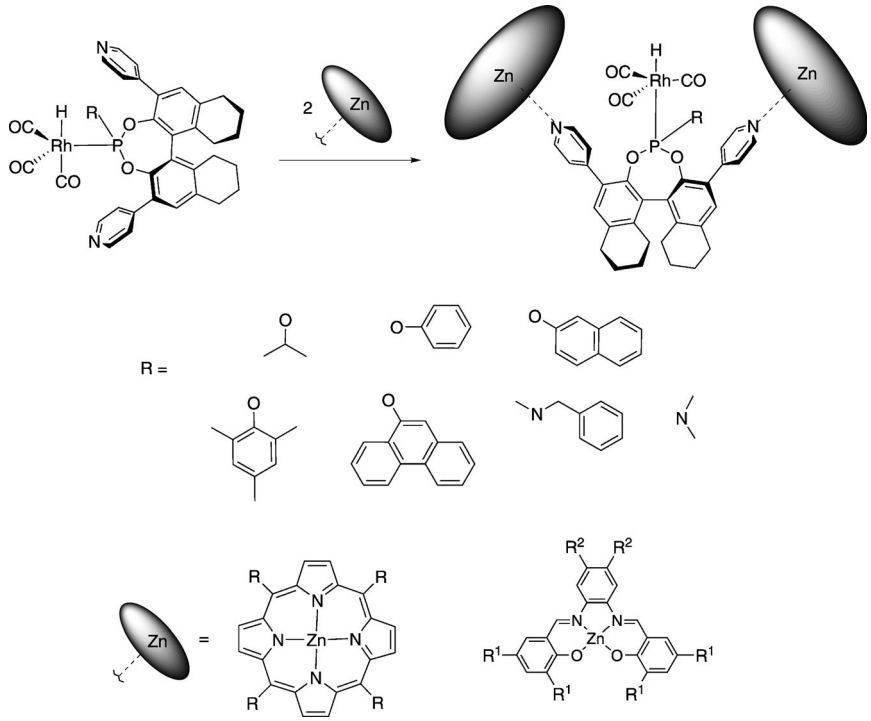

Figure 2. General structure of the shift of pyridine-based monodentate ligands upon addition of Zn^{II}-template to a rhodium complex.

Spectroscopic experiments on such systems indicate that only one bulky phosphite ligand coordinates to the metal centre in the equatorial plane, *cis* to the hydride. Along the same lines, Breit and co-workers have reported the use of bulky phosphabenzenes in hydroformylation catalysis.[9] In situ HP NMR and IR analyses indicated that the active and selective catalyst was a monophosphabenzene rhodium complex in which the ligand is located in the equatorial plane.

Recently, we have introduced a ligand-template approach for the supramolecular encapsulation of transition-metal complexes.[10] Ligand-template tris-3-pyridyl phosphine coordinate Zn^{II}-porphyrins exclusively through the nitrogen donor atom, whereas the phosphorus atom coordinates to the catalytically active rhodium. The rhodium complex formed under hydroformylation conditions has only one phosphorus atom coordinated in the equatorial position, and this catalytic system displayed unprecedented regioselectivity in the hydroformylation of unfunctionalised terminal and internal alkenes. In this contribution, we report the use of chiral pyridyl-phosphoramidite and phosphite ligands that, in the presence of Zn^{II}-building blocks, show remarkable supramolecular control on the coordination mode of the rhodium hydroformylation complex.[11] The coordination of the phosphorus to rhodium changes from equatorial to axial in the presence of a supramolecular template. The supramolecular change is reflected in higher activity and enantioselectivity when these complexes were applied to the very challenging asymmetric hydroformylation of unfunctionalised internal alkenes. We report our investigations into the origin of this shift in ligand coordination on a rhodium hydroformylation complex, and evaluate possible steric and electronic effects induced by Zn^{II}-templates by evaluating a series of ligand-template building blocks (Figure 2). Consistent control of the ligand coordination in a rhodium hydroformylation catalyst from the *cis* to *trans* position after addition of the Zn^{II}-template is observed, and in the asymmetric hydroformylation of internal alkenes this *trans* complex displayed higher activity, higher enantioselectivity, as well as an increase in regioselectivity compared with the analogous *cis* catalyst.

Results and Discussion

Ligand Synthesis: The ligands were synthesised starting from commercially available (*S*)-2,2′-binaphthol, which was reduced in the presence of Pd/C. The diol **2** obtained was selectively brominated in the 3,3′-position at low temperature (−30 °C) to give compound **3**. Suzuki coupling of **3** with the appropriate boronic acid provided intermediates **4a** and **4b**, which were treated with $P(NMe_2)_3$ and 4-(*N*,*N*-dimethylamino)pyridine (DMAP) in toluene at reflux to give ligands (*S*)-**1a** and (*S*)-**1b** in good yield (Scheme 1).

Following the second route depicted in Scheme 2, ligands (*S*)-**1c**–**h** were synthesised. The ligands were prepared in a two-step fashion starting from diol **4a**, which, after reaction with PCl_3, gave phosphorochloridite **5**. Condensation of a range of nucleophiles with **5** afforded the corresponding

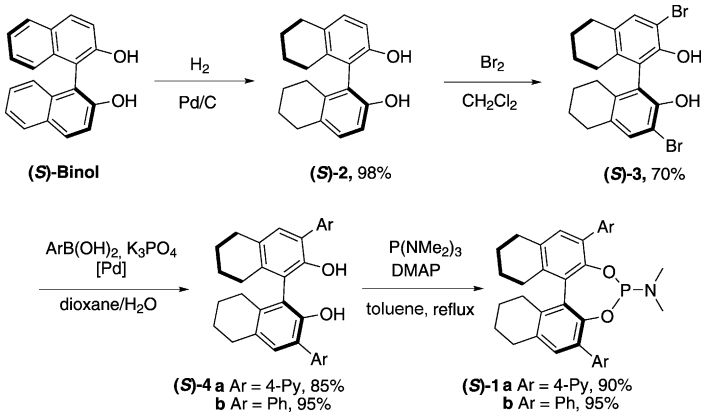

Scheme 1. Synthesis of phosphoroamidite ligands.

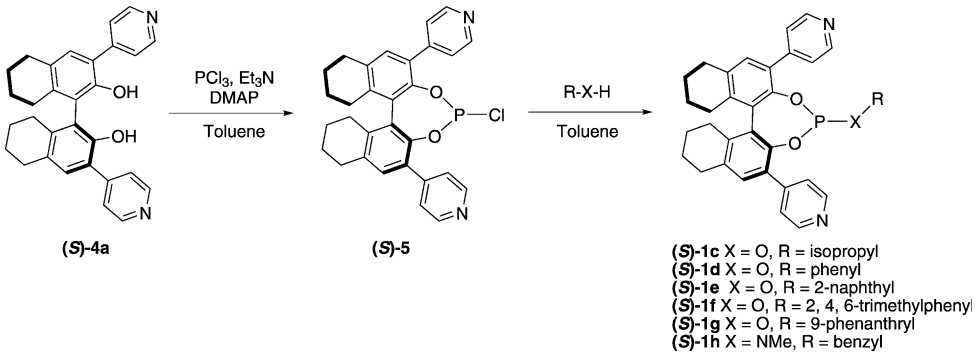

Scheme 2. General synthesis of the pyridine-based monodentate ligands.

phosphite and phosphoroamidite ligands **1c–h** in good yield.[12,13] All new compounds were fully characterised by ^{1}H NMR, ^{31}P NMR and ^{13}C NMR spectroscopy and by mass spectroscopic analysis.

Coordination studies: *The assembly of ligand (S)-1a and Zn^{II}-tetraphenylporphyrin 6*: The coordination behaviour of ligand (*S*)-**1a** towards Zn^{II}-tetraphenylporphyrin **6** was investigated by NMR and UV/Vis spectroscopy. The UV/Vis titration experiments revealed binding constants of $K_1 = 1.8\times10^3\,\text{M}^{-1}$ and $K_2 = 1.7\times10^3\,\text{M}^{-1}$, related to the first and second association of porphyrin to (*S*)-**1a** (Scheme 3). The similarity between these constants indicates that the binding events are independent and that no cooperativity is present as previously observed in the case of tris-3-pyridyl phosphine.[10b] A job-plot analysis indicated the formation of a 1:2 complex between the phosphoroamidite ligand **1a** and the template **17** (see Figure 4 below).[13] The binding of this building block through the nitrogen donor atom is very selective, implying that the phosphorus atom of the ligand is available for coordination to the transition-metal centre.

In situ high-pressure NMR and IR analyses: The coordination behaviour of (*S*)-**1a** to rhodium under catalytically relevant conditions was studied using high-pressure (HP) NMR and IR spectroscopy. Rhodium complexes were prepared in situ by using [Rh(acac)CO$_2$] as the metal precursor in [D$_8$]toluene under 5 bar syngas (H$_2$/CO, 1:1) (Scheme 4). The complex based on bulky ligand (*S*)-**1a** is monoligated [Rh(H)(CO)$_3$**1a**], with the phosphorus ligand in the equatorial position; a hydride signal centred at $\delta = -11.01$ ppm is observed with a small PH coupling consistent with the *cis*-[Rh(H)(CO)$_3$**1a**] complex. Interestingly, in the presence of two equivalents of porphyrin **6**, the HP ^{1}H NMR spectrum revealed new signals in the hydride region; a double doublet centred at $\delta = -10.3$ ppm with a large phosphorus coupling [J(P,H) = 180 Hz and J(Rh,H) =

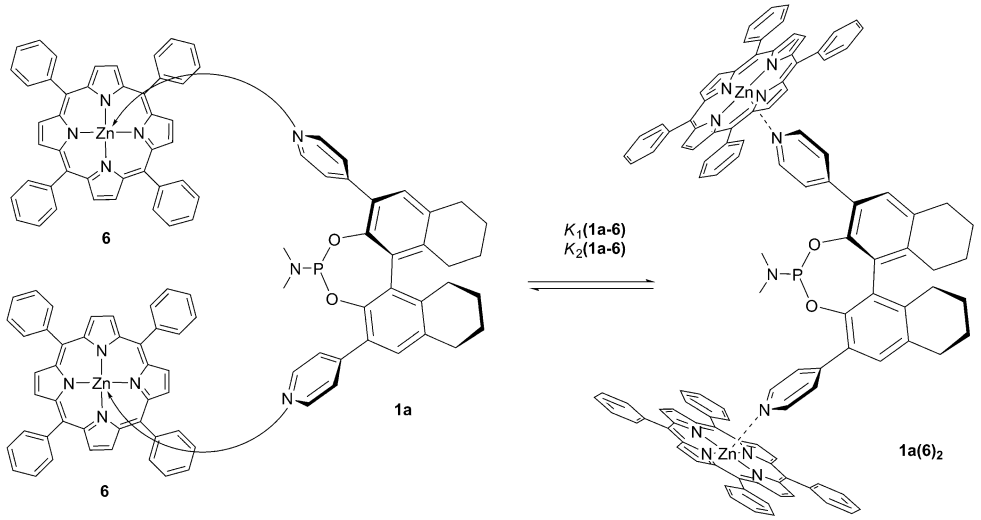

Scheme 3. Assembly of ligand (*S*)-**1a** on Zn^{II}-tetraphenylporphyrin **6**.

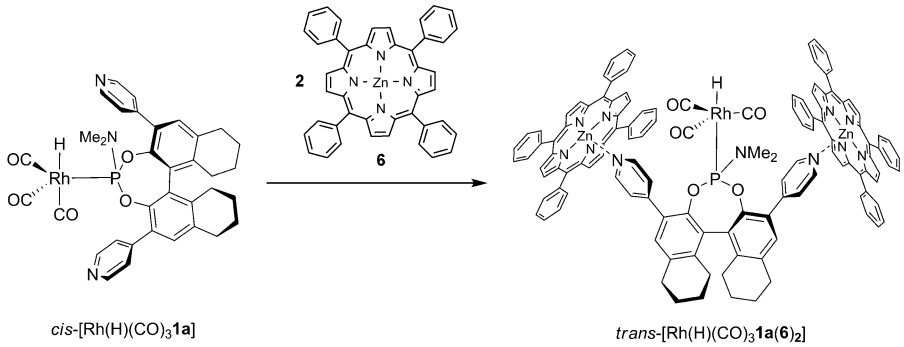

Scheme 4. Structures of *cis*-[Rh(H)(CO)$_3$**1a**] and *trans*-[Rh(H)(CO)$_3$**1a**(**6**)$_2$] derived from the high-pressure ^{1}H NMR spectra.

6.1 Hz] indicating the formation of the *trans*-[Rh(H)(CO)$_3$**1a**(**6**)$_2$] complex. Further experiments such as HP ^{1}H-{^{31}P}-NMR and 2D ^{1}H-^{31}P NMR spectroscopic studies confirmed the formation of the rhodium complex in which the supramolecular monodentate ligand is coordinated *trans* to the hydride.[13]

The formation of complexes *cis*-[Rh(H)(CO)$_3$**1a**] and *trans*-[Rh(H)(CO)$_3$**1a**(**6**)$_2$] were investigated under actual hydroformylation conditions by IR spectroscopy, using reaction conditions and concentrations identical to those applied in catalysis.[13] In the presence of [Rh(acac)CO$_2$] and ligand (*S*)-**1a**, the tris-carbonyl rhodium hydride complex *cis*-[Rh(H)(CO)$_3$**1a**] was obtained, as shown by the three peaks in the carbonyl region of the IR spectrum at 2054, 2000 and 1982 cm^{-1}. The rhodium complex formed in the presence of (*S*)-**1a** and two equivalents of porphyrin **6** shows three absorption bands that are shifted to higher wavenumbers (2055, 2022 and 1998 cm^{-1}).[13] These higher wavenumbers indicate weaker π-back-donation to the CO molecules in the *trans*-[Rh(H)(CO)$_3$**1a**(**6**)$_2$] complex and, hence, CO dissociation from this assembly should be faster. If CO dissociation is involved in the rate determining step, as is commonly observed for phosphine-based catalysis, this could lead to an increase in reaction rates.

To determine whether this unusual coordination mode is more general, we also investigated the coordination properties of ligands (*S*)-**1c–h** by HP NMR analysis. Rhodium complexes were prepared in situ by using [Rh(acac)(CO)$_2$] in [D$_8$]toluene under 5 bar syngas (H$_2$/CO, 1:1), and fully characterised by HP ^{1}H NMR, HP ^{31}P NMR, HP ^{1}H-{^{31}P}-NMR and HP 2D ^{1}H-^{31}P NMR analyses, confirming the formation of the rhodium complexes.[13] In line with our previous observations, all these new ligands showed a switching in coordination mode upon addition of the supramolecular template. This supramolecular control over ligand coordination therefore appears to be rather general.

Influence of steric and electronic properties on the *trans* rhodium-complex: To determine whether this unusual template effect is due to the steric bulk of the Zn^{II}-templates, we carried out HP NMR experiments using the much smaller template triethylborane (BEt$_3$) in combination with ligand (*S*)-**1a**. The HP ^{1}H NMR and ^{31}P NMR spectra showed formation of a rhodium complex in which the phosphoroamidite ligand was located *trans* to the hydride, indicating that the size of the template is not responsible for the switching of ligand coordination.[13]

To probe the electronic influence of the Zn^{II}-template in changing the electron density on the pyridine moiety and therefore on the phosphorus donor atom, we performed IR studies using several Zn^{II}-templates (Figure 3). Zn^{II}-templates containing more electron-withdrawing substituents will increase the electron-withdrawing capacity of the pyridine ring, which should result in a lower basicity of the phosphorus atom. Ligand (*S*)-**1a** and [Rh(acac)CO$_2$] were mixed in a 1:1 ratio to form [Rh(**1a**)CO(acac)] in situ and, subsequently, two equivalents of Zn^{II}-template were added. The IR spectra of these rhodium complexes show that the addition of the Zn^{II}-template shifts the stretching of the carbonyl (ν_{CO} = 1999.6 cm^{-1}) of [Rh(**1a**)CO(acac)] to higher wavenumbers. This indicates a lower electron density on the rhodium, which implies decreased back-bonding from the metal to the carbonyl ligand, and hence higher CO stretch-

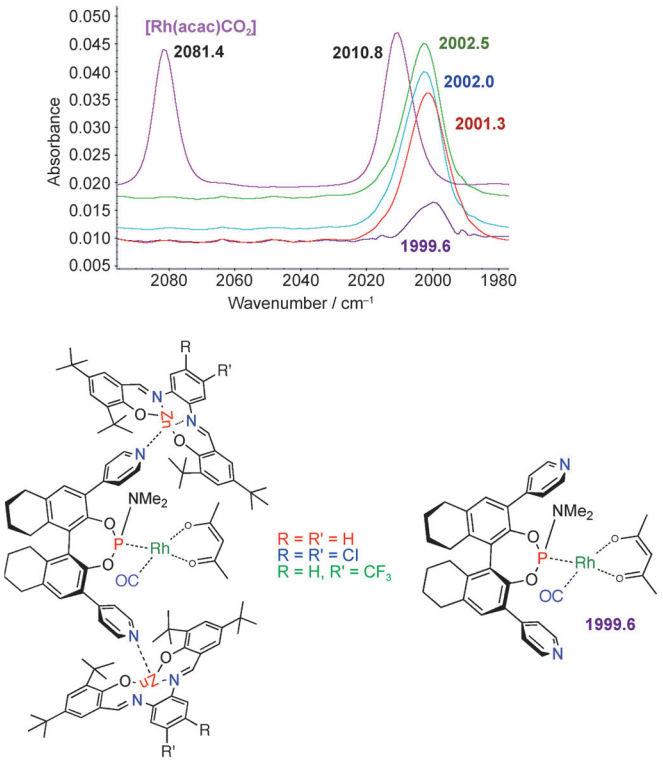

Figure 3. IR spectra of ligand (*S*)-**1a** acquired in the presence of different Zn^{II}-salphens.

ing frequencies are observed. More electron-withdrawing substituents on the Zn^{II}-templates gives higher ν_{CO}-band frequency, which shows that the electronic properties of the phosphoroamidite ligands can indeed be influenced by the Zn^{II}-templates.[13]

Application of the supramolecular ligands in asymmetric hydroformylation: Catalyst performances of *cis*- and *trans*-complexes based on ligands (*S*)-**1a**–**h** and template **6** (Zn^{II}-tetraphenylporphyrin) as well as some control ligands such as PPh_3, (*R*,*S*)-Binaphos and (*S*)-**1b** were investigated in the asymmetric hydroformylation (AHF) of *trans*-2-octene **7a** (Scheme 5).[14,15]

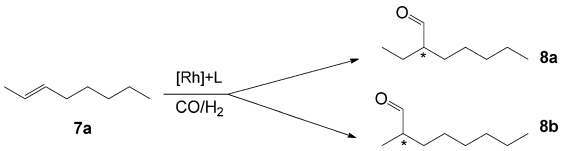

Scheme 5. Hydroformylation of *trans*-2-octene.

As expected, the rhodium catalyst derived from triphenylphosphine gave only low conversions and a significant amount of isomerisation (Table 1, entry 1). The rhodium catalyst based on (*R*,*S*)-Binaphos (Table 1, entry 2) gave useful conversion (55%) but no significant enantiomeric excess.

Complex [Rh(H)(CO)$_3$**1a**] yielded the product with an enantiomeric excess of 25%, albeit with relatively low conversion (12%; Table 1, entry 5). Interestingly, in the presence of template **6**, and thus with complex [Rh(H)(CO)$_3$**1a**(**6**)$_2$], an increase in both conversion (56%) and enantioselectivity (45%) was observed (Table 1, entry 6). This indicates that the change in coordination mode improves the catalyst performance in this challenging reaction both in terms of activity and selectivity. Control experiments using ligand (*S*)-**1b** (Table 1, entries 3 and 4), which lacks the pyridyl group, shows that these complexes give rise to low activity and the product **8a** is produced in low enantiomeric excess, regardless of the presence of Zn^{II}-porphyrin **6**. Further indications of the absence of any effects of the Zn^{II}-template in the presence of ligand (*S*)-**1b** were obtained by IR studies and high-pressure NMR experiments.[13] No changes in the spectra were observed upon addition of the Zn^{II}-template to the rhodium catalyst binding ligand (*S*)-**1b**. This demonstrates that template **6** does not interfere directly with the rhodium-catalysed hydroformylation.

Table 1. Results of the asymmetric hydroformylation of *trans*-2-octene.[a]

Entry	Ligand	Conv. [%][b]	Iso. [%][c]	**8a**/**8b**[b,d]	**8a** *ee* [%][e,f]
1	PPh_3	6	5	0.8	0
2	(*R*,*S*) Binaphos	55	4	0.7	0
3	(*S*)-**1b**	12	4	0.7	11 (*R*)
4	(*S*)-**1b**, **6** (2 equiv)	11	4	0.6	10 (*R*)
5	(*S*)-**1a**	12	4	0.7	25 (*R*)
6	(*S*)-**1a**(**6**)$_2$	56	0	1.0	45 (*R*)
7	(*S*)-**1c**	13	4	0.9	8 (*R*)
8	(*S*)-**1c**(**6**)$_2$	37	2	1.9	30 (*R*)
9	(*S*)-**1d**	15	5	0.9	8 (*R*)
10	(*S*)-**1d**(**6**)$_2$	98	1	2.1	19 (*R*)
11	(*S*)-**1e**	12	1	0.8	4 (*R*)
12	(*S*)-**1e**(**6**)$_2$	72	0	2.0	13 (*R*)
13	(*S*)-**1f**	91	1	0.9	8 (*R*)
14	(*S*)-**1f**(**6**)$_2$	99	2	1.4	24 (*R*)
15	(*S*)-**1g**	85	0	0.8	4 (*R*)
16	(*S*)-**1g**(**6**)$_2$	97	0	1.2	20 (*R*)
17	(*S*)-**1h**	32	3	1.1	20 (*R*)
18	(*S*)-**1h**(**6**)$_2$	25	0	2.3	45 (*R*)

[a] Reagents and conditions: [Rh] = 1 mM in toluene, ligand/rhodium = 9, *trans*-2-octene/rhodium = 200, 25 °C, 20 bar, 84 h. [b] Percentage conversion determined by GC analysis. [c] Percentage of alkene isomerisation product. [d] Ratio of the products **8a** and **8b**. [e] Enantiomeric excess of product **8a**. [f] The absolute configuration was determined by comparing the GC traces with those of the enantiopure aldehydes (*R*)-**8a** and (*S*)-**8a**.[11]

Having established that the supramolecular ligand (*S*)-**1a**(**6**)$_2$ performed better in terms of activity and selectivity, we explored the use of different phosphite and phosphoroamidite pyridyl-based ligands (*S*)-**1c**–**h** and their assemblies with template **6** in the same reaction. The results show a similar trend; an increase in activity and selectivity was observed in the presence of templated ligands (Table 1, entries 8, 10, 12, 14, 16 and 18). In general, the use of bulky phosphite ligands led to higher conversions, especially when employing catalysts based on supramolecular ligands **1d**(**6**)$_2$, **1f**(**6**)$_2$ and **1g**(**6**)$_2$ (Table 1, entries 10, 14 and 16). Interestingly, increasing the steric bulk at the phosphorus atom led to an increase in regioselectivity for the inner aldehyde **8a** (Table 1, entries 8, 10, 12, 14, 16 and 18). With the current set of ligands it was possible to tune the **8a**/**8b** ratio between 0.7 and 2.3, which is quite an achievement considering the symmetry of the substrate.

In further studies we explored a small series of boron- and zinc-based templates (Figure 4) in combination with ligand (*S*)-**1a**, aiming to further fine-tune the properties of the supramolecular ligands. Remarkably, the properties of the template had very little effect on the catalyst properties; in all cases the enantiomeric excess increased from 25%, observed for the catalyst based on the parent ligand, to 35–42% for the various templated ligands (Table 2, entries 1 vs. 2–8). Because we even observed this increase in enantiomeric excess for the smallest boron-based templates **11** and **12** (Table 2, entries 2 and 3), we conclude that the dominant effect on enantioselectivity is associated with the change in coordination mode of the ligand, switching from equatorial to axial upon templation. In terms of regioselectivity (**8a**/**8b** ratio) and conversion also only small effects were noted upon changing the template.

Influence of reaction conditions: *Syngas pressure*: The influence of syngas pressure was investigated by performing a series of experiments at 10, 20, 30 and 40 bar (H_2/CO = 1:1), using *trans*-[Rh(H)(CO)$_3$**1a**(**6**)$_2$] and *cis*-[Rh(H)(CO)$_3$**1a**] complexes and *trans*-2-octene as substrate

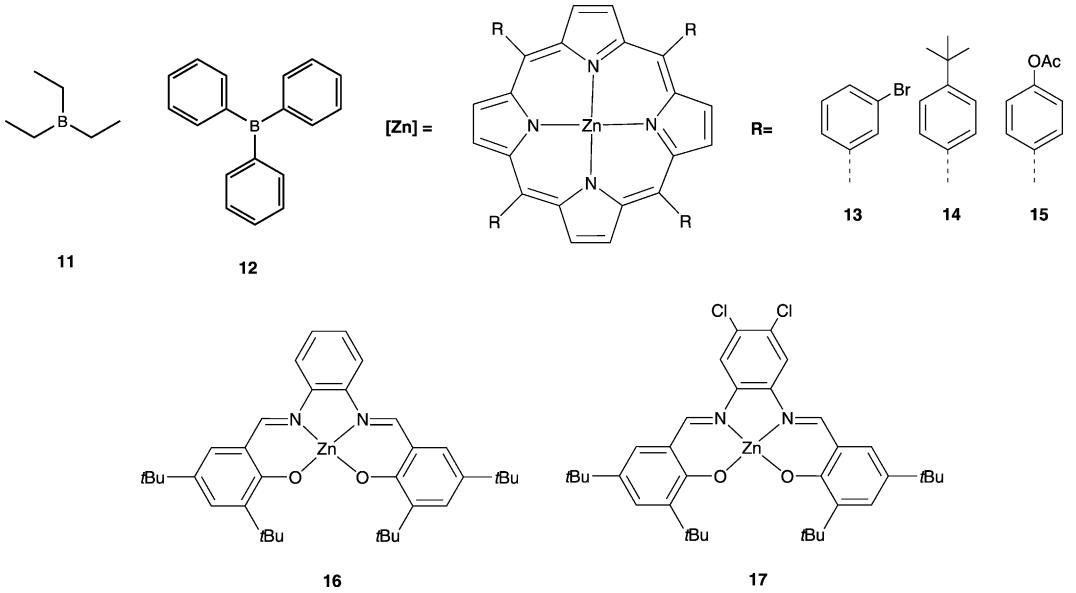

Figure 4. Boron- and zinc-based building blocks.

Table 2. Asymmetric hydroformylation of *trans*-2-octene; screening of boron and zinc-templates in combination with ligand (*S*)-**1a**.[a]

Entry	Ligand	Conv. [%][b]	Iso. [%][c]	**8a**/**8b**[b,d]	**8a** *ee* [%][e,f]
1	(*S*)-**1a**	12	4	0.7	25 (*R*)
2	(*S*)-**1a**(**11**)$_2$	30	0.6	0.9	35 (*R*)
3	(*S*)-**1a**(**12**)$_2$	30	1.0	0.8	41 (*R*)
4	(*S*)-**1a**(**13**)$_2$	43	0.6	0.9	37 (*R*)
5	(*S*)-**1a**(**14**)$_2$	52	0.6	1.0	41 (*R*)
6	(*S*)-**1a**(**15**)$_2$	52	0.6	1.0	41 (*R*)
7	(*S*)-**1a**(**16**)$_2$	51	0.7	1.1	42 (*R*)
8	(*S*)-**1a**(**17**)$_2$	53	0	1.1	35 (*R*)

[a] Reagents and conditions: [Rh] = 1 mM in toluene, ligand/rhodium = 9, *trans*-2-octene/rhodium = 200, 25 °C, 20 bar, 84 h. [b] Percentage conversion determined by GC analysis. [c] Percentage of alkene isomerisation product. [d] Ratio of the products **8a** and **8b**. [e] Enantiomeric excess of product **8a**. [f] The absolute configuration was determined by comparing the GC traces with those of the enantiopure aldehydes (*R*)-**8a** and (*S*)-**8a**.[11]

Table 3. Results of the asymmetric hydroformylation of *trans*-2-octene.[a]

Entry	Ligand	H_2/CO	*T* [°C]	Conv. [%][b]	Iso. [%][c]	**8a**/**8b**[d]	**8a** *ee* [%][e,f]
1	**1a**	5:5	25	28	5.0	0.7	28 (*R*)
2	**1a**(**6**)$_2$	5:5	25	58	1.0	0.9	41 (*R*)
3	**1a**	10:10	25	38	4.1	0.7	26 (*R*)
4	**1a**(**6**)$_2$	10:10	25	54	0.5	1.0	43 (*R*)
5	**1a**	15:15	25	30	2.1	0.7	28 (*R*)
6	**1a**(**6**)$_2$	15:15	25	49	0	1.0	43 (*R*)
7	**1a**	20:20	25	27	2.1	0.7	27 (*R*)
8	**1a**(**6**)$_2$	20:20	25	43	0	1.0	43 (*R*)
9	**1a**	20:10	25	31	3.2	0.7	26 (*R*)
10	**1a**(**6**)$_2$	20:10	25	47	1.2	1.0	48 (*R*)
11	**1a**	10:20	25	15	1.1	0.7	24 (*R*)
12	**1a**(**6**)$_2$	10:20	25	15	0.5	1.0	45 (*R*)
13	**1a**	10:20	50	>99	2	0.7	14 (*R*)
14	**1a**(**6**)$_2$	10:20	50	>99	0	1.0	27 (*R*)
15	**1a**	10:10	50	>99	1	0.7	15 (*R*)
16	**1a**(**6**)$_2$	10:10	50	>99	0	0.9	25 (*R*)

[a] Reagents and conditions: [Rh] = 1 mM in toluene, ligand/rhodium = 5, *trans*-2-octene/rhodium = 200, 25 °C, 20 bar, 84 h. [b] Percentage conversion determined by GC analysis. [c] Percentage of alkene isomerisation product. [d] Ratio of the products **8a** and **8b**. [e] Enantiomeric excess of product **8a**. [f] The absolute configuration was determined by comparing the GC traces with those of the enantiopure aldehydes (*R*)-**8a** and (*S*)-**8a**.[11]

(Table 2). Under all pressure conditions, complex *trans*-[Rh(H)(CO)$_3$**1a**(**6**)$_2$] displayed higher activity and selectivity than *cis*-[Rh(H)(CO)$_3$**1a**] (Table 3, entries 1–8). As expected for rhodium complexes that follow type I kinetics[3] (negative order in CO), an increase in pressure results in a drop in conversion and a decrease in isomerisation. No changes in enantioselectivity were observed with any of the catalysts using different reaction pressures. The optimal pressure for the application of *trans*-[Rh(H)(CO)$_3$**1a**(**6**)$_2$] was 20 bar; under these conditions, the isomerisation side reaction was slow and the conversion was good (Table 3, entry 4).

We examined the effect of CO and H_2 partial pressures and found that varying the hydrogen pressure had little effect on either activity or selectivity, which is typical for type I kinetics (Table 3, entries 9 and 10). Hydroformylation with higher ratios of CO pressure led to a decrease in conversion but did not affect the chemo- or enantioselectivity (Table 3, entries 11 and 12). Increasing the reaction temperature to 50 °C under these pressure conditions resulted in full conversion but also lower enantioselectivity (Table 3, entry 13 and 14). Increasing the reaction temperature to 50 °C under standard pressure conditions of 20 bar also led to higher conversions, a slight increase in isomerisation and lower enantiomeric excess (Table 3, entries 15 and 16).

The remaining catalytic reactions were conducted under the conditions that gave the optimum compromise between

enantioselectivities and reaction rates: a total pressure of 20 bar of syngas, a temperature of 25 °C and a ratio of CO/H_2 of 1:1.

Influence of the ligand/rhodium ratio: We next studied the effect of the supramolecular monodentate ligand (*S*)-**1a**(**6**)$_2$/rhodium ratio. Usually, an excess of ligand is required to prevent ligand-free rhodium complexes being formed. Ligand/rhodium ratios from 1:1 to 9:1 were explored. At low ligand concentrations, low selectivity and high conversion was observed (Table 4, entry 1), indicating the formation of rhodium hydride tris-carbonyl species, which is known to be highly reactive under these conditions.[3] Increasing the ligand concentration provided a catalyst system that displayed higher enantioselectivity (Table 4, entries 2–6). Increasing the ligand/metal ratio to more than 2:1 (at these concentrations) did not produce any significant changes in selectivity of the catalyst, showing that a small excess of ligand is sufficient to transform all the rhodium into the ligated, catalytically active species.

Table 4. Results of the asymmetric hydroformylation of *trans*-2-octene by using different ratios of ligand (*S*)-**1a**(**6**)$_2$ to rhodium.[a]

Entry	**1a**(**6**)$_2$/Rh	Conv. [%][b]	Iso. [%][c]	**8a**/**8b**[d]	**8a** *ee* [%][e,f]
1	1	91	11	0.6	0
2	2	36	3	1.0	44 (*R*)
3	3	39	1	1.1	47 (*R*)
4	5	40	1	1.1	46 (*R*)
5	7	40	1	1.1	45 (*R*)
6	10	42	1	1.1	46 (*R*)

[a] Reagents and conditions: [Rh] = 1 mM in toluene, *trans*-2-octene/rhodium = 200, 25 °C, 20 bar, 84 h. [b] Percentage conversion determined by GC analysis. [c] Percentage of alkene isomerisation product. [d] Ratio of the products **8a** and **8b**. [e] Enantiomeric excess of product **8a**. [f] The absolute configuration was determined by comparing the GC traces with those of the enantiopure aldehydes (*R*)-**8a** and (*S*)-**8a**.[11]

Influence of the Zn^{II}-template/ligand ratio: To obtain more insight into the templated ligand effect, we studied the formation of the rhodium complexes using different ratios of template **6** to ligand (*S*)-**1a**. In Figure 5 the enantioselectivity obtained as a function of the **6**/**1a** ratio is displayed. Interestingly, a major increase in enantioselectivity was already observed using a **6**/**1a** ratio of 1:1. From the experiments above it was clear that the dominant effect in the change of selectivity is the change in coordination mode. These experiments together suggest that the formation of the rhodium-hydride complex in which the phosphorus is *trans* to the hydride already occurs if one the two templates is coordinated to the ligand. High-pressure NMR experiments with the complex based on a 1:1 ratio of template **6** to ligand (*S*)-**1a** indeed confirm the quantitative formation of the *trans*-[Rh(H)(CO)$_3$**1a**-(**6**)] complex under these conditions.[13] The enantiomeric excess slightly increased between a ratio of 1:1 and 1:2, but no further changes in the catalysis were observed upon addition of more than two equivalents of template **6**.

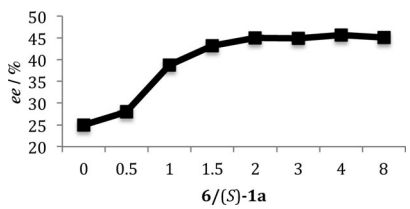

Figure 5. Enantioselectivity of **8a** formed in the rhodium-catalysed asymmetric hydroformylation of *trans*-2-octene by using (*S*)-**1a** in the presence of various amounts of Zn^{II}-template **6**.

Asymmetric hydroformylation of *trans*-2-alkenes: To see if the unusual template effect is more general, we investigated the AHF of a series of *trans*-2-alkenes. In Table 5 we report the results obtained using catalytic complexes *cis*-[Rh(H)(CO)$_3$**1a**] and *trans*-[Rh(H)(CO)$_3$**1a**(**6**)$_2$] in the presence of *trans*-2-alkenes. As observed for *trans*-2-octene, these substrates are also produced with higher enantioselectivity when the templated ligand **1a**(**6**)$_2$ is used (Table 5, entries 2, 4 and 6) compared with the nontemplated analogue (Table 5, entries 1, 3 and 5). Ligands (*S*)-**1c–h** were also applied in the AHF of these substrates, and these experiments also show higher enantio- and regioselectivity when the templated ligands were employed (see the Supporting Information for details).

Table 5. Results of the asymmetric hydrofomylation of internal alkenes by using ligand (*S*)-**1a** and template **6**.[a]

Entry	Alkene	Template	Conv. [%][b]	Iso. [%][c]	**10a**/**10b**[d]	**10a** *ee* [%][e]
1	(*E*)-2-hexene	–	23	2	0.7	21
2	(*E*)-2-hexene	**6**	65		0.9	46
3	(*E*)-2-heptene	–	22	1	0.7	26
4	(*E*)-2-heptene	**6**	43		1.0	44
5	(*E*)-2-nonene	–	40		0.7	23
6	(*E*)-2-nonene	**6**	52		1.0	47

[a] Reagents and conditions: [Rh] = 1 mM in toluene, ligand/rhodium = 3, *trans*-2-octene/rhodium = 200, 25 °C, 20 bar, 84 h. [b] Percentage conversion determined by GC analysis. [c] Percentage of alkene isomerisation product. [d] Ratio of the products **10a** and **10b**. [e] Enantiomeric excess of product **10a**. For detailed conditions see the Supporting Information.

Complexes *cis*-[Rh(H)(CO)$_3$**1a**] and *trans*-[Rh(H)(CO)$_3$**1a**(**6**)$_2$] were also tested in the asymmetric hydroformylation of a small series of *cis*-2-alkenes. Although, higher conversions were achieved with the supramolecular system, the enantioselectivities were not always higher for the templated complex.[13]

Conclusion

Our results demonstrate that for monodentate pyridine-containing phosphoroamidite and phosphite ligands, the coordi-

nation mode to rhodium can be controlled in a unique supramolecular fashion. In situ high-pressure NMR and IR studies under hydroformylation conditions show for the first time the formation of rhodium-hydride complexes in which the phosphorus donor atom of the ligand is *trans* to the hydride, but only after coordination of Zn^{II}-templates (or Boron based) to the pyridyl moieties of the ligand. In the absence of these Zn^{II}-templates, typical monoligated rhodium-hydrido complexes are formed with the ligand in the equatorial plane, in *cis* orientation to the hydride. The origin of this shift in ligand coordination is not steric in nature, because the size of the template does not influence this shift in coordination mode. Moreover, the size of the template also does not affect the catalytic outcome; in all cases, a similar increase in conversion and enantioselectivity compared to the *cis* rhodium complex was observed. Instead, electronic effects induced by the Zn^{II}-templates on the phosphorus donor atom are most likely responsible, as supported by IR spectroscopic studies. These newly developed phosphite and phosphoroamidite ligands proved to be effective ligands in rhodium-catalysed asymmetric hydroformylation of generally unreactive internal unfuctionalised alkenes leading to high conversion and moderate enantioselectivity. The results also reveal that the presence of sterically bulky groups on the phosphorus moiety significantly improved the regioselectivity of this challenging reaction. Further studies are focussed on extending this concept to other reactions, and further improving the enantio- and regioselectivity of this reaction.

Experimental Section

General methods: Unless stated otherwise, reactions were carried out under an atmosphere of argon using standard Schlenk techniques. NMR spectra (^1H, ^{31}P and ^{13}C) were measured with a Bruker DRX 400 MHz or an Inova 500 MHz; $CDCl_3$ was used as solvent, if not further specified. High-resolution mass spectra were recorded with a JEOL JMS SX/SX102 A four-sector mass spectrometer; for FAB-MS, 3-nitrobenzyl alcohol was used as matrix. UV/Vis spectroscopy experiments were performed with a Cary UV/Vis System. Gas chromatographic analyses were run with a Shimadzu GC-17 A apparatus (split/splitless injector, J&W Scientific, DB-1 J&W 30 m column, film thickness 3.0 μm, carrier gas 70 kPa He, FID Detector). Chiral GC separations were conducted with an Interscience HR GC apparatus with a Supelco β-dex 225 capillary column. Details of the synthesis of (*S*)-**1a** and (*S*)-**1b** were reported in previous work.[8]

Preparation of ligands (*S*)-5: In a flame-dried Schlenk flask (*S*)-**4a** (200 mg, 0.44 mmol), pyridine (0.034 mL, 0.44 mmol) and DMAP (10 mol%) were suspended in anhydrous toluene (4.4 mL, 0.1 M). The solution was cooled to 0 °C and distilled PCl_3 (0.080 mL, 0.88 mmol) was added dropwise over 10 min. The mixture was allowed to warm to RT and then heated to reflux overnight. The reaction mixture was cooled to RT and the formation of product was checked by ^{31}P NMR analysis. The solvent and the residual PCl_3 were removed in vacuum and the resulting solid was used for the next step without any further purification.

General procedure for the preparation of ligands (*S*)-1c–h: In a flame-dried Schlenk flask, nucleophile (0.44 mmol) and pyridine (0.040 mL, 0.48 mmol) were dissolved in anhydrous toluene (1 mL). The solution was added dropwise to a cooled (0 °C) mixture of (*S*)-**5** (225.7 mg, 0.44 mmol) in anhydrous toluene (5 mL). The mixture was allowed to warm to RT and stirred overnight at this temperature. The precipitate formed was filtered through a pad of Celite and the solvent was evaporated in vacuum to obtain (*S*)-**1c**, (*S*)-**1d**, (*S*)-**1e**, (*S*)-**1f**, (*S*)-**1g**, and (*S*)-**1h**.

Ligand (*S*)-1c: Yield: 51% (0.23 mmol); white foam; ^1H NMR (400 MHz, [D$_8$]toluene): $\delta = 8.66$ (m, 4H), 8.44 (m, 4H), 7.06 (s, 1H), 7.01 (s, 1H), 2.68 (m, 4H), 2.29 (m, 2H), 2.13 (m, 1H), 1.62 (m, 8H), 1.34 (m, 2H), 0.74 (d, $J = 6.7$ Hz, 3H), 0.51 ppm (d, $J = 6.7$ Hz, 3H); ^{13}C NMR (400 MHz): $\delta = 149.4$ (CH), 146.3 (C), 145.3 (C), 143.9 (C), 139.1 (C), 138.4 (C), 134.6 (C), 133.6 (CH), 124.2 (CH), 69.3 (CH), 28.8 (CH_2), 27.6 (CH_2), 23.7 (CH_3), 23.1 (CH_3), 22.8 (CH_2), 0.82 ppm (CH); ^{31}P NMR (400 MHz): $\delta = 145.4$ ppm. HRMS (FAB+): *m/z* calcd for $C_{33}H_{34}N_2O_3P$: 537.2306 $[M+H]^+$; found: 537.2307.

Ligand (*S*)-1d: Yield: 56% (0.25 mmol); white foam; ^1H NMR (400 MHz, $CDCl_3$): $\delta = 8.65$ (m, 2H), 8.57 (m, 2H), 7.57 (m, 2H), 7.51 (m, 2H), 7.22 (m, 2H), 7.06 (m, 1H), 6.98 (m, 2H), 6.22 (m, 2H), 2.92 (m, 4H), 2.77 (m, 2H), 2.47 (m, 2H), 1.90 ppm (m, 8H); ^{13}C NMR (400 MHz): $\delta = 149.3$ (CH), 148.9 (C), 139.7 (C), 138.9 (C), 137.8 (C), 135.7 (C), 135.0 (C), 129.5 (CH), 129.0 (CH), 124.7 (CH), 124.4 (CH), 124.1 (CH), 119.0 (CH), 118.9 (CH), 115.3 (CH), 29.3 (CH_2), 29.23 (CH_2), 22.4 ppm (CH_2); ^{31}P NMR (400 MHz): $\delta = 140.8$ ppm. HRMS (FAB+): *m/z* calcd for $C_{36}H_{32}N_2O_3P$: 571.2154 $[M+H]^+$; found: 571.2151.

Ligand (*S*)-1e: Yield: 77% (0.34 mmol); white foam; ^1H NMR (400 MHz, $CDCl_3$): $\delta = 8.63$ (m, 2H), 8.52 (m, 2H), 7.59 (m, 1H), 7.51 (m, 2H), 7.40 (m, 3H), 7.25 (m, 3H), 6.98 (m, 1H), 6.61 (s, 1H), 6,54 (s, 1H), 6,52 (s, 1H), 2.70 (m, 4H), 2.39 (m, 2H), 2.16 (m, 2H), 1.66 ppm (m, 8H); ^{13}C NMR (400 MHz): $\delta = 154.4$ (C), 149.3 (CH), 148.7 (C), 146.6 (C), 139.7 (C), 135.7 (C), 133.6 (C), 130.4 (C), 129.9 (CH), 129.1 (CH), 129.2 (C), 128.2 (CH), 127.5 (CH), 126.8 (CH), 124.7 (CH), 123.2 (CH), 119.8 (CH), 118.3 (CH), 115.1 (CH), 109.4 (CH), 29.3 (CH_2), 28.0 (CH_2), 22.6 (CH_2), 22.4 ppm (CH_2); ^{31}P NMR (400 MHz): $\delta = 135.5$ ppm. HRMS (FAB+): *m/z* calcd for $C_{40}H_{33}N_2O_3P$: 621.2229 $[M+H]^+$; found: 621.2217.

Ligand (*S*)-1f: Yield: 86% (0.38 mmol); white foam; ^1H NMR (400 MHz, $CDCl_3$): $\delta = 8.60$ (d, $J = 5.6$ Hz, 2H), 8.55 (d, $J = 5.6$ Hz, 2H), 7.60 (d, $J = 5.5$ Hz, 2H), 7.49 (d, $J = 5.5$ Hz, 2H), 7.21 (s, 1H), 7.18 (s, 1H), 6.81 (s, 1H), 6.65 (s, 1H), 2.93 (m, 4H), 2.74 (m, 2H), 2.45 (m, 2H), 2.17 (s, 3H), 1.90 (m, 8H), 1.64 ppm (s, 6H); ^{13}C NMR (400 MHz): $\delta =$ 135.4 (C), 134.5 (C), 133.8 (C), 130.2 (CH), 130.2 (CH), 129.7 (C), 129.4 (C), 129.3 (CH), 129.2 (CH), 124.9 (CH), 124.5 (CH), 29.7 (CH_2), 29.1 (CH_2), 27.8 (CH_2), 22.5 (CH_2), 22.4 (CH_3), 16.6 (CH_3), 15.8 ppm (CH_3); ^{31}P NMR (400 MHz): $\delta = 139.8$ ppm. HRMS (FAB+): *m/z* calcd for $C_{39}H_{37}N_2O_3P$: 613.2542 $[M+H]^+$; found: 513.2544.

Ligand (*S*)-1g: Yield: 43% (0.19 mmol); white foam; ^1H NMR (400 MHz, [D$_8$]toluene): $\delta = 8.64$ (m, 4H), 8.53 (m, 2H), 8.40 (m, 2H), 8.22 (m, 2H), 7.69 (m, 2H), 7.45 (m, 4H), 6.48 (s, 1H), 6.37 (s, 1H), 2.71 (m, 4H), 2.59 (m, 2H), 2.46 (m, 2H), 1.66 ppm (m, 8H); ^{13}C NMR (400 MHz): $\delta = 155.4$ (C), 149.7 (CH), 145.6 (C), 136.2 (C), 135.2 (C), 134.6 (C), 130.3 (CH), 128.7 (CH), 127.9 (CH), 126.8(CH), 125.4 (CH), 124.2 (CH), 122.6 (CH), 122.4 (CH), 122.3 (CH), 105.5 (CH), 29.3 (CH_2), 29.0 (CH_2), 22.5 (CH_2), 22.3 ppm (CH_2); ^{31}P NMR (400 MHz): $\delta =$ 140.0 ppm. HRMS (FAB+): *m/z* calcd for $C_{44}H_{35}N_2O_3P$: 671.2385 $[M+H]^+$; found: 671.2474.

Ligand (*S*)-1h: Yield: 53% (0.23 mmol); white foam; ^1H NMR (400 MHz, $CDCl_3$): $\delta = 8.68$ (m, 4H), 7.63 (m, 2H), 7.56 (m, 2H), 8.02 (m, 2H), 7.27–7.20 (m, 5H), 6.91 (m, 2H), 2.92 (m, 4H), 2.74 (m, 2H), 2.38 (m, 2H), 1.88 (m, 8H), 1.81 (s, 3H), 1.72 (s, 3H), 1.28 ppm (s, 3H); ^{13}C NMR (400 MHz): $\delta = 149.6$ (CH), 149.4 (C), 148.1 (C), 145.3 (C), 139.0 (C), 134.0 (C), 129.6 (CH), 128.3 (CH), 127.3 (CH), 126.9 (CH), 124.5 (CH), 124.0 (CH), 29.4 (CH_2), 27.9 (CH_2), 22.4 (CH_2), 0.89 ppm (CH_3); ^{31}P NMR (400 MHz): $\delta = 138.2$ ppm. HRMS (FAB+): *m/z* calcd for $C_{38}H_{36}N_3O_2P$: 598.2623 $[M+H]^+$; found: 598.2620.

General procedure for the rhodium-catalysed hydroformylation: A typical experiment was carried out in a stainless steel autoclave (150 mL) charged with an insert suitable for 14 reaction vessels (equipped with Teflon mini stirring bars) for performing parallel reactions. Each vial was charged with Zn^{II}-template (10 μmol, 10 equiv), ligand (5 μmol, 5 equiv), [Rh(acac)CO$_2$] (1 μmol), substrate (0.03 mL, 20 μmol) and toluene

(1 mL). The substrate was filtered over basic alumina to remove possible peroxide impurities. Toluene was distilled from sodium prior to use. Before starting the catalysis, the charged autoclave was purged three times with 10 bar of syngas (H_2/CO = 1:1) and then pressurised to 20 bar. After the catalytic reaction, the autoclave was cooled to 0 °C, the pressure was reduced to 1.0 bar and a few drops of tri-*n*-butyl-phosphite were added to each reaction vessel to prevent any further reaction. The reaction mixtures were not filtered over basic alumina to remove catalyst residues because filtration may cause retention of the aldehydes and thus influence the results of the GC analysis. The mixtures were diluted with CH_2Cl_2 for GC analysis. The absolute configuration was determined by comparing the chiral GC traces of the reaction mixture to the enantiopure aldehydes (*S*)-2-ethylheptanal and (*R*)-2-ethylheptanal obtained by known methods.[11]

Preparation of the hydride complexes for high-pressure NMR analysis: A solution of pyridine-based ligand (1 equiv), Zn^{II}-template (2 equiv) and [Rh(acac)CO_2] in [D_8]toluene (20 mM) was stirred at 40 °C for 3 h. The mixture was then transferred to a 5 mm HP NMR tube, pressurised with 5 bar of syngas (H_2/CO, 1:1) at 40 °C for 24 h and the high-pressure NMR spectra were recorded.

Preparation of the hydride complexes for high-pressure IR analysis: High-pressure IR experiments were performed in an SS-316 50 mL autoclave equipped with IRTRAN windows (ZnS, transparent above 700 cm^{-1}, ø = 10 mm, optical path length = 0.4 mm), a mechanical stirrer, temperature controller, and a pressure device. In a typical experiment, the high-pressure IR autoclave was filled with (*S*)-**1a** (33 mg, 0.063 mmol), Zn^{II}-tetraphenylporphyrin **6** (85 mg, 0.126 mmol) and dichloromethane (13 mL). The autoclave was purged three times with 15 bar of H_2/CO (1:1) and pressurised to 20 bar. The antichamber was charged with a solution of [Rh(acac)CO_2] (2.7 mg, 0.01 mmol) in dichloromethane (2 mL) and pressurised to 30 bar. The HP-IR autoclave was placed into a Nicolet 510 FTIR spectrometer and the temperature was set to 40 °C. When the desire temperature was reached, the antichamber was opened and the catalyst precursor was injected into the solution. The series of IR spectra was recorded for 24 h, during which time the samples were stirred.

Acknowledgements

We thank Dr. S. H. Chikkali and Dr. G. Berthon-Gelloz for valuable discussions and suggestions. This work was financially supported by the National Research School Combination Chemistry (NRSCC) and by the European Union, Marie-Curie ITN *RevCat*.

[1] a) C. A. Tolman, *Chem. Rev.* **1977**, *77*, 313–348; b) C. A. Tolman, *J. Am. Chem. Soc.* **1970**, *92*, 2953–2956; c) C. P. Casey, G. T. Whiteker, *Isr. J. Chem.* **1990**, *30*, 299–304; d) P. W. N. M. van Leeuwen, P. C. J. Kamer, J. N. H. Reek, P. Dierkes, *Chem. Rev.* **2000**, *100*, 2741–2769.

[2] a) P. C. J. Kamer, A. van Rooy, G. C. Schoemaker, P. W. N. M. van Leeuwen, *Coord. Chem. Rev.* **2004**, *248*, 2409–2424; b) C. Kubis, R. Ludwig, M. Sawall, K. Neymeyr, A. Börner, K. D. Wiese, D. Hess, R. Franke, D. Selent, *ChemCatChem* **2010**, *2*, 287–295.

[3] P. W. N. M. van Leeuwen and C. Claver, in *Rhodium-Catalyzed Hydroformylation*, Kluwer Academic Publishers, Dordrecht, **2000** and references cited therein.

[4] a) M. Kranenburg, Y. E. M. van der Burgt, P. C. J. Kamer, P. W. N. M. van Leeuwen, *Organometallics* **1995**, *14*, 3081–3089; b) L. A. van der Veen, P. H. Keeven, G. C. Schoemaker, J. N. H. Reek, P. C. J. Kamer, P. van Leeuwen, M. Lutz, A. L. Spek, *Organometallics* **2000**, *19*, 872–883.

[5] a) S. Deerenberg, P. C. J. Kamer, P. W. N. M. van Leeuwen, *Organometallics* **2000**, *19*, 2065–2072; b) O. Pàmies, G. Net, A. Ruiz, C. Claver, *Tetrahedron: Asymmetry* **2001**, *12*, 3441–3445; c) M. Rubio, A. Suárez, E. Álvarez, C. Bianchini, W. Oberhauser, M. Peruzzini, A. Pizzano, *Organometallics* **2007**, *26*, 6428–6486; d) Y. Yan, X. Zhang, *J. Am. Chem. Soc.* **2006**, *128*, 7198–7201; e) S. Chikkali, R. Bellini, G. Berthon-Gelloz, J. I. van der Vlugt, B. de Bruin, J. N. H. Reek, *Chem. Commun.* **2010**, *46*, 1244–1246; f) X. Zhang, B. Cao, Y. Yan, S. Yu, B. Ji, X. Zhang, *Chem. Eur. J.* **2010**, *16*, 871–877; g) T. Robert, Z. Abiri, J. Wassenaar, A. J. Sandee, S. Romanski, J. M. Neudörfl, H. G. Schmalz, J. N. H. Reek, *Organometallics* **2010**, *29*, 478–483; h) J. Wassenaar, B. de Bruin, J. N. H. Reek, *Organometallics* **2010**, *29*, 2767–2776; i) G. Franciò, F. Faraone, W. Leitner, *Angew. Chem.* **2000**, *112*, 1486–1488; *Angew. Chem. Int. Ed.* **2000**, *39*, 1428–1430.

[6] a) K. Nozaki, N. Sakai, T. Nanno, T. Higashijima, S. Mano, T. Horiuchi, H. Takaya, *J. Am. Chem. Soc.* **1997**, *119*, 4413–4423; b) K. Nozaki, T. Matsuo, F. Shibahara, T. Hiyama, *Organometallics* **2003**, *22*, 594–600; c) D. A. C. Molina, C. P. Casey, I. Müller, K. Nozaki, C. Jäkel, *Organometallics* **2010**, *29*, 3362–3367.

[7] a) A. J. Minnaard, B. L. Feringa, L. Lefort and J. G. de Vries, *Acc. Chem. Res.* **2007**, *40*, 1267–1277; b) M. T. Reetz, *Angew. Chem.* **2008**, *120*, 2592–2626; *Angew. Chem. Int. Ed.* **2008**, *47*, 2556–2588; c) J. F. Teichert, B. L. Feringa, *Angew. Chem.* **2010**, *122*, 2538–2582; *Angew. Chem. Int. Ed.* **2010**, *49*, 2486–2528; d) C. Gennari and U. Piarulli, *Chem. Rev.* **2003**, *103*, 3071–3100; e) T. Jerphagnon, J.-L. Renaud, C. Bruneau, *Tetrahedron: Asymmetry* **2004**, *15*, 2101–2111; f) D. W. Norman, D. J. Hyett, P. G. Pringle, J. B. Sweeney, A. G. Orpen, H. Phetmung and R. Wingad, *J. Am. Chem. Soc.* **2008**, *130*, 6840–6847; g) C. Monti, C. Gennari, U. Piarulli, J. G. de Vries, A. H. M. de Vries, L. Lefort, *Chem. Eur. J.* **2005**, *11*, 6701–6717.

[8] P. W. N. M. van Leeuwen, C. F. Roobeek, *J. Organomet. Chem.* **1983**, *258*, 343–350.

[9] B. Breit, R. Winde, T. Mackewitz, R. Paciello, K. Harms, *Chem. Eur. J.* **2001**, *7*, 3106–3121.

[10] a) V. F. Slagt, J. N. H. Reek, P. C. J. Kamer, P. W. N.M van Leeuwen, *Angew. Chem.* **2001**, *113*, 4401–4404; *Angew. Chem. Int. Ed.* **2001**, *40*, 4271–4274; b) V. F. Slagt, P. C. J. Kamer, P. W. N. M. van Leeuwen, J. N. H. Reek, *J. Am. Chem. Soc.* **2004**, *126*, 1526–1536; c) M. Kuil, T. Solter, P. W. N. M. van Leeuwen, J. N. H. Reek, *J. Am. Chem. Soc.* **2006**, *128*, 11344–11345; d) A. W. Kleij, M. Kuil, D. M. Tooke, A. L. Spek, J. N. H. Reek, *Inorg. Chem.* **2005**, *44*, 7696–7698; e) A. W. Kleij, M. Lutz, A. L. Spek, P. W. N. M. van Leeuwen, J. N. H. Reek, *Chem. Commun.* **2005**, 3661–3663; f) A. W. Kleij, J. N. H. Reek, *Chem. Eur. J.* **2006**, *12*, 4219–4227.

[11] For a preliminary communication, see: R. Bellini, S. H. Chikkali, G. Berthon-Gelloz, J. N. H. Reek, *Angew. Chem.* **2011**, *123*, 7480–7483; *Angew. Chem. Int. Ed.* **2011**, *50*, 7342–7345.

[12] a) N. Kudo, M. Perseghini, G. C. Fu, *Angew. Chem.* **2006**, *118*, 1304–1306; *Angew. Chem. Int. Ed.* **2006**, *45*, 1282–1284; b) C. J. O'Brien, E. A. B. Kantchev, C. Valente, N. Hadei, G. A. Chass, A. Lough, A. C. Hopkinson, M. G. Organ, *Chem. Eur. J.* **2006**, *12*, 4743–4748; c) M. Bartoszek, M. Beller, J. Deutsch, M. Klawonn, A. Kockritz, N. Nemati, A. Pews-Davtyan, *Tetrahedron* **2008**, *64*, 1316–1322; d) G. Erre, K. Junge, S. Enthaler, D. Addis, D. Michalik, A. Spannenberg, M. Beller, *Chem. Asian J.* **2008**, *3*, 887–894.

[13] For details see the Supporting Information.

[14] For hydroformylation, see: a) B. Breit, W. Seiche, *Synthesis* **2001**, 1–36; b) B. Breit, *Top. Curr. Chem.* **2007**, *279*, 139–172; c) Z. Hua, V. C. Vassar, H. Choi, I. Ojima, *Proc. Natl. Acad. Sci. USA* **2004**, *101*, 5411–5416; d) B. Breit, E. Fuchs, *Chem. Commun.* **2004**, 694–695; e) E. Fuchs, M. Keller and B. Breit, *Chem. Eur. J.* **2006**, *12*, 6930–6939; f) M. L. Clarke, *Current Org. Chem.* **2005**, *9*, 701–718; g) N. Sakai, K. Nozaki, and H. Takaya, *J. Chem. Soc., Chem. Commun.* **1994**, 395–396; h) R. I. McDonald, G. W. Wong, R. P. Neupane, S. S. Stahl, C. R. Landis, *J. Am. Chem. Soc.* **2010**, *132*, 14027–14029.

[15] For alternative supramolecular control, see: a) T. Šmejkal, B. Breit, *Angew. Chem.* **2008**, *120*, 317–321; *Angew. Chem. Int. Ed.* **2008**, *47*, 311–315; *Angew. Chem.* **2008**, *120*, 4010–4013; *Angew. Chem. Int. Ed.* **2008**, *47*, 3946–3949; b) P. Dydio, W. Dzik, M. Lutz, B. de Bruin, J. N. H. Reek, *Angew. Chem.* **2011**, *123*, 416–420; *Angew. Chem. Int. Ed.* **2011**, *50*, 396–400.

Received: January 20, 2012
Published online: ■■ ■■, 2012

Asymmetric Hydroformylation

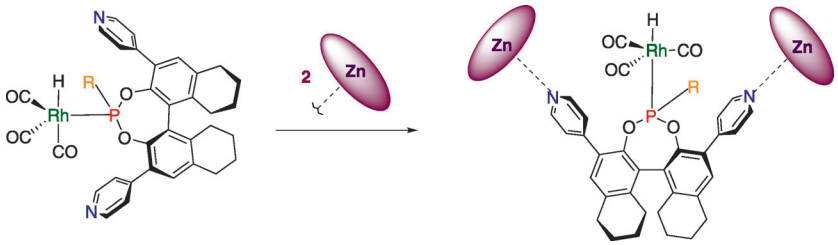

A guiding hand: The coordination mode of monodentate phosphoroamidite and phosphite ligands in a rhodium hydroformylation complex can be switched from equatorial to axial mode by a unique supramolecular pseudo encapsulation (see scheme). The supramolecular axial complex displays higher activity and selectivity in the challenging asymmetric hydroformylation of internal alkenes.